Electronic Supplementary Information (ESI)

Simple Mechanisms of CH_4 Reforming with CO_2 and H_2O on Supported Ni/ZrO_2 Catalyst

Hui Yang,[†,‡,§] Hui Wang,[†,‡,§] Lisha Wei,[†,‡,§] Yong Yang,[†,‡] Yong-Wang Li,[†,‡] Xiao-dong Wen*[,†,‡] and Haijun Jiao*[,‖]

[†]State Key Laboratory of Coal Conversion, Institute of Coal Chemistry, Chinese Academy of Sciences, Taiyuan, 030001, China.
[‡]National Energy Center for Coal to Liquids, Synfuels China Co., Ltd, Huairou District, Beijing, 101400, China
[§]University of Chinese Academy of Sciences, No. 19A Yuquan Road, Beijing, 100049, China
[‖]Leibniz-Institut für Katalyse e.V., Albert-Einstein-Str. 29a, Rostock, 18059, Germany

Table of Contents

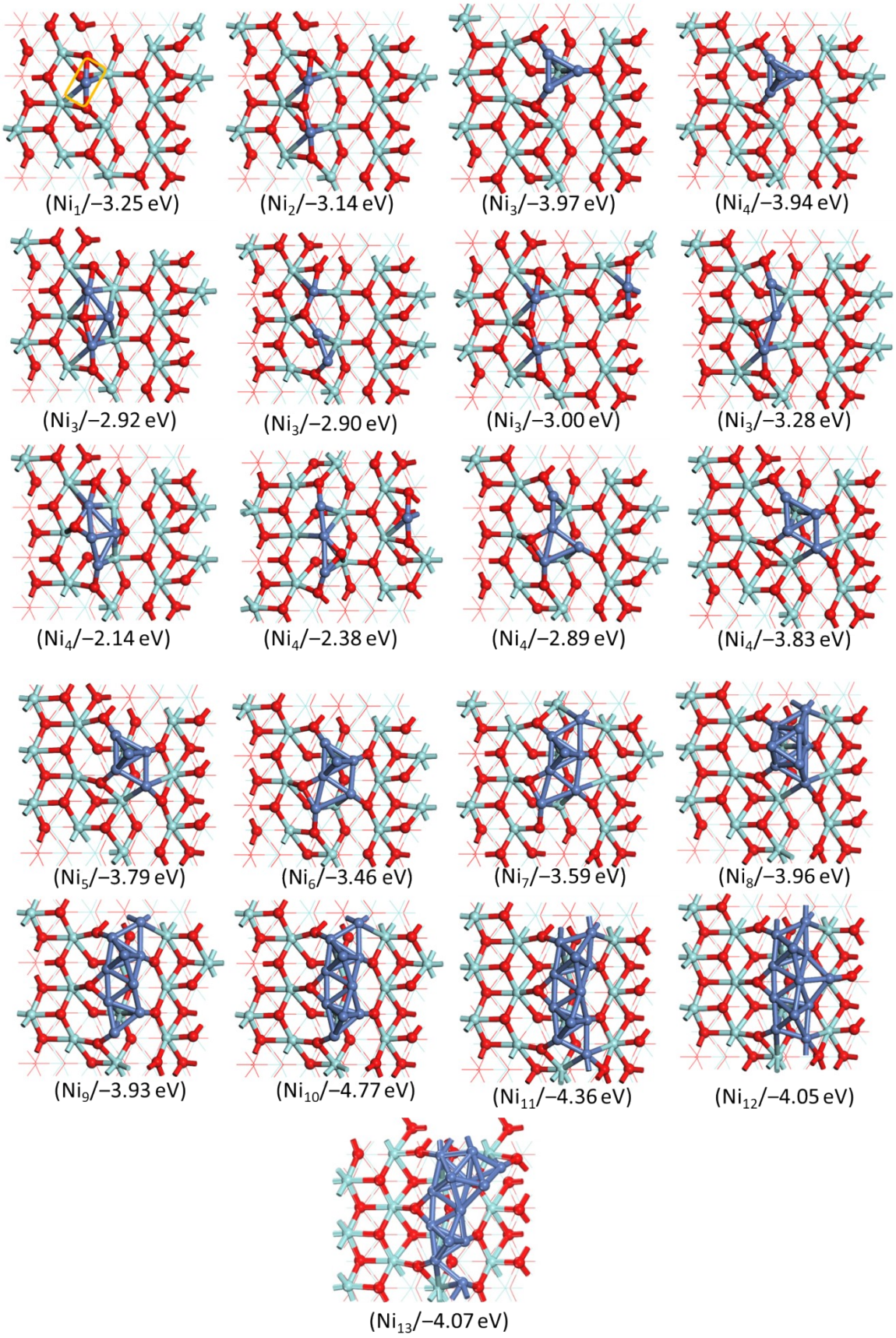

Figure S1. Stable adsorption structures of Ni_n (n = 1-13) on t-ZrO_2(101) with the sequential adsorption energy in parenthesis (white-blue, red and blue balls for Zr, O and Ni atoms, respectively)

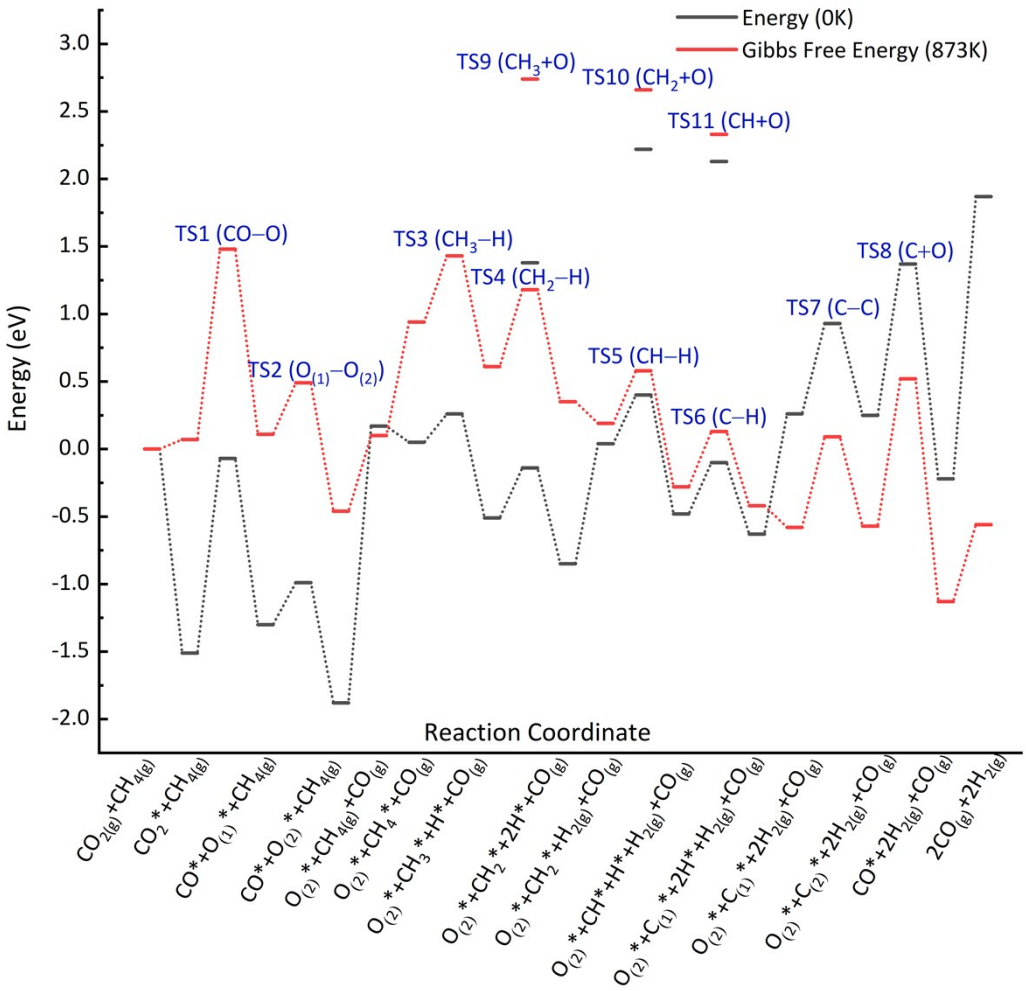

Figure S2. Energy profile of possible pathway for CO_2 reforming of CH_4 on Ni_{13}/*t*-ZrO_2(101) from DFT calculation (0 K and 1 bar) with ZPE correction (black line) and Gibbs free energy profile (873 K and 1bar) (red line)

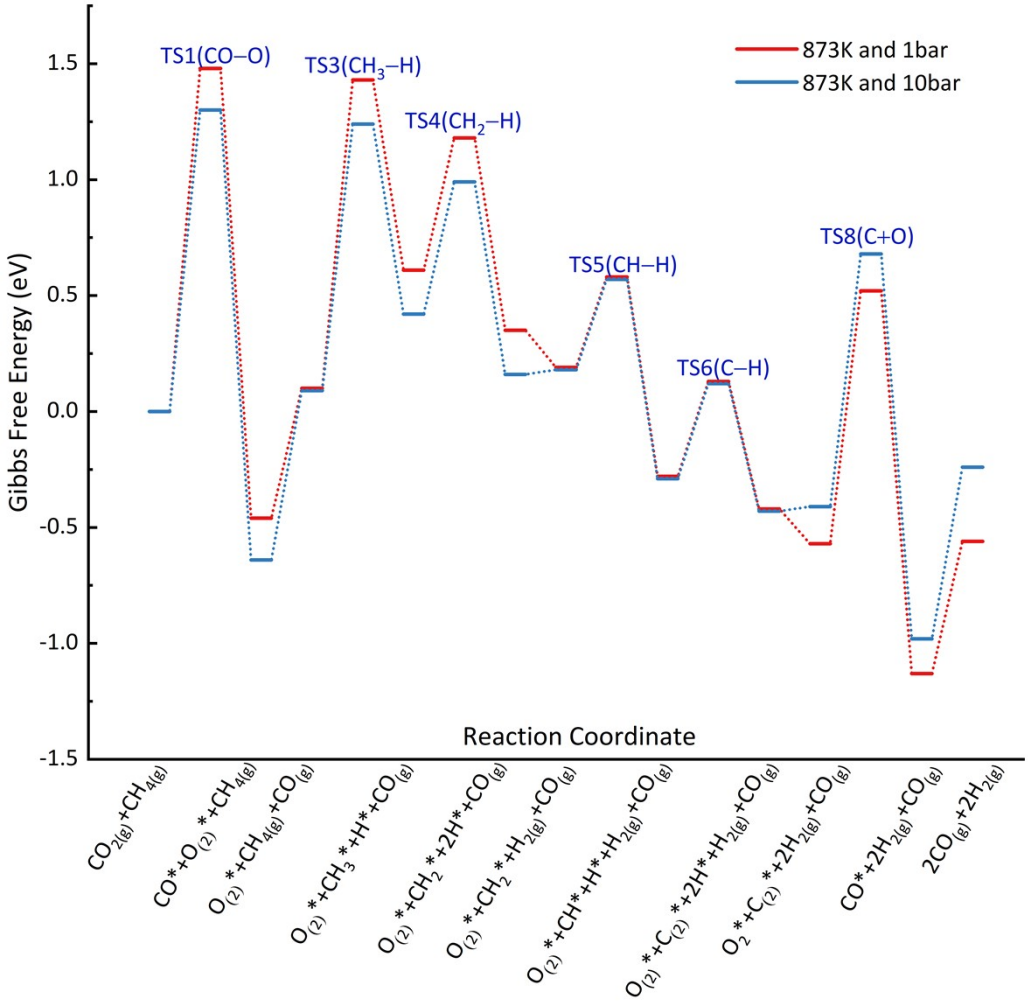

Figure S3. Simplified Gibbs free energy profile of CO_2 reforming of CH_4 on Ni_{13}/*t*-ZrO_2(101) under 873K with 1bar (red line) and 873K with 10bar (blue line) conditions, respectively.

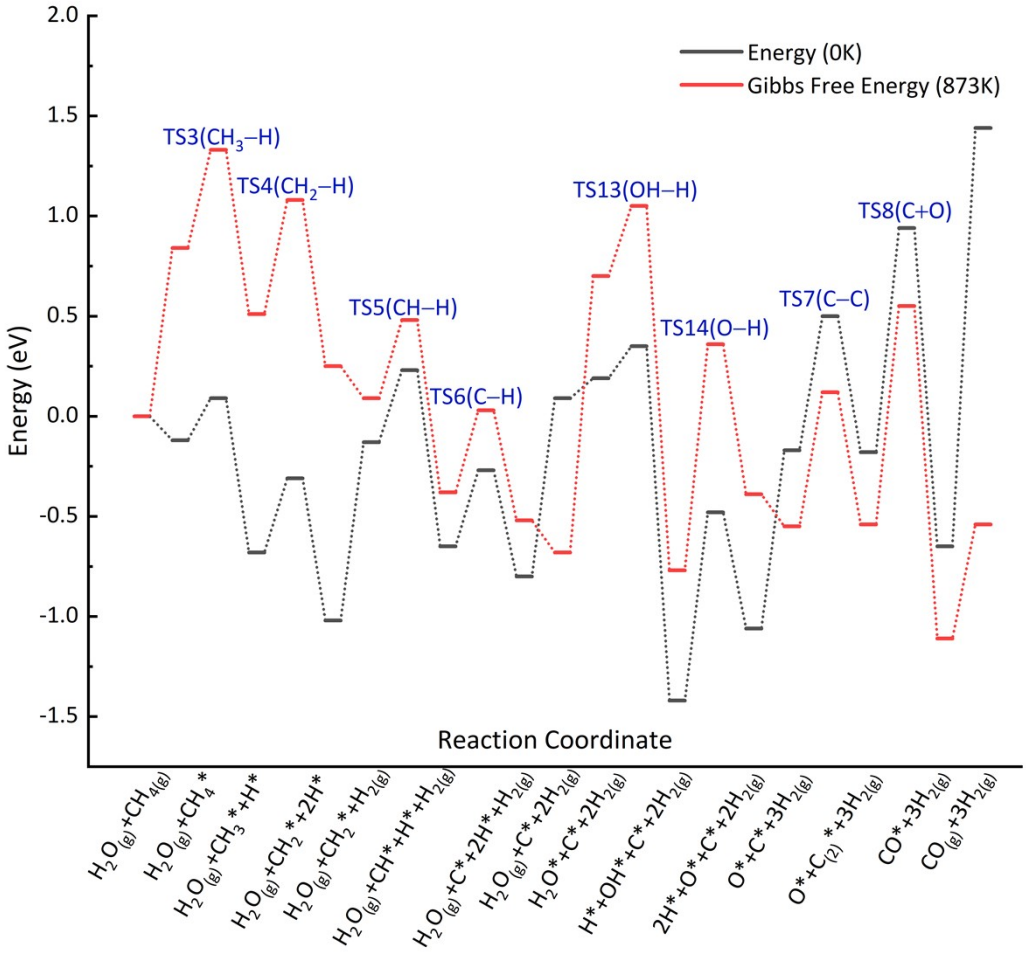

Figure S4. Potential Energy surface of possible pathway for steam reforming of CH_4 on Ni_{13}/*t*-ZrO_2(101) from DFT calculation (0 K and 1 bar) with ZPE correction (black line) and the Gibbs free energy profile (873 K and 1bar) (red line)

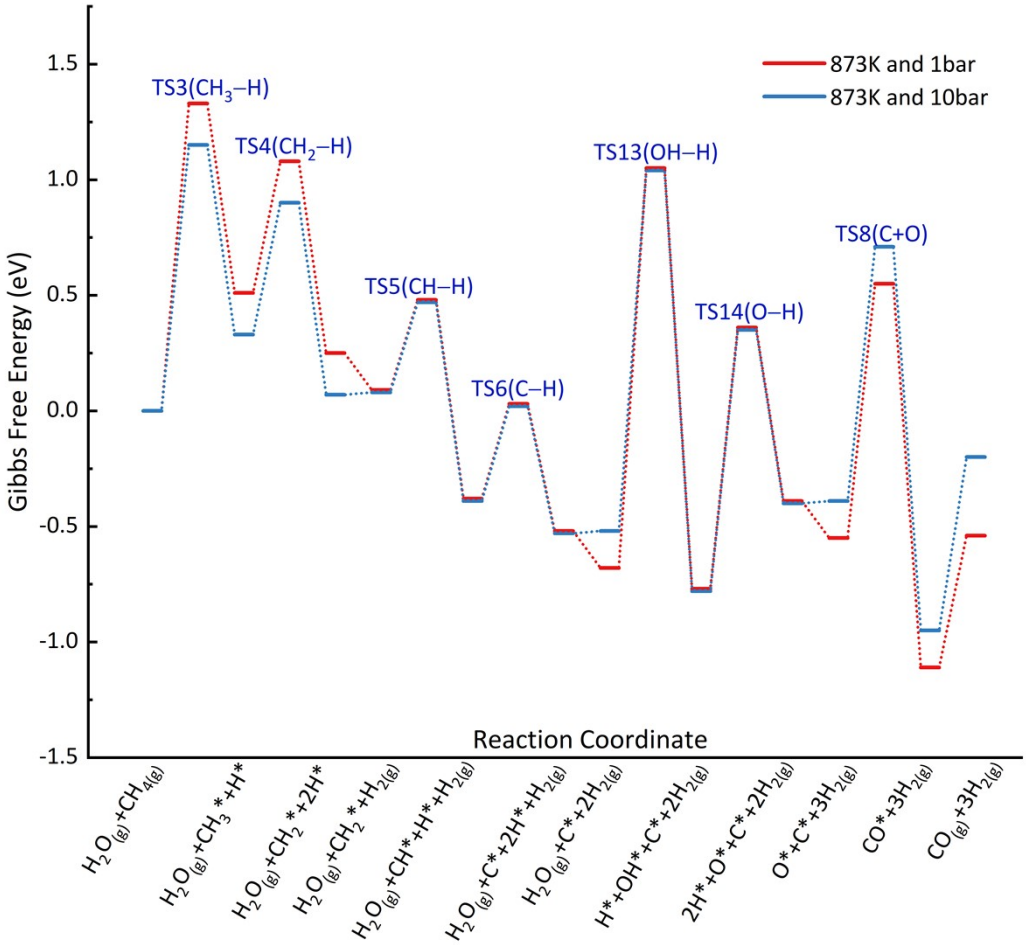

Figure S5. Simplified Gibbs free energy profile of H_2O reforming of CH_4 on Ni_{13}/*t*-ZrO_2(101) under 873K with 1bar (red line) and 873K with 10bar (blue line) conditions, respectively.

TableS1. Forward reaction rate constant (*k*, s^{-1}) for elementary reactions in methane reforming on Ni/*t*-ZrO_2 catalyst under different conditions.

Reactions	TS	*k* (873K; 1bar)	*k* (873K; 10bar)	*k* (873K; 30bar)	*k* (973K;10bar)
$CO_2 \rightarrow CO+O$	TS1	5.56×10^{04}	6.03×10^{05}	1.74×10^{06}	5.89×10^{05}
$O_{(1)} \rightarrow O_{(2)}$	TS2	1.18×10^{11}	1.18×10^{11}	1.18×10^{11}	1.75×10^{11}
$CH_4 \rightarrow CH_3+H$	TS3	4.05×10^{05}	4.40×10^{06}	1.27×10^{07}	5.01×10^{06}
$CH_3 \rightarrow CH_2+H$	TS4	9.56×10^{09}	9.56×10^{09}	9.56×10^{09}	1.62×10^{10}
$CH_2 \rightarrow CH+H$	TS5	1.04×10^{11}	1.04×10^{11}	1.04×10^{11}	1.75×10^{11}
$CH \rightarrow C+H$	TS6	7.96×10^{10}	7.96×10^{10}	7.96×10^{10}	1.38×10^{11}
$C_{(1)} \rightarrow C_{(2)}$	TS7	2.54×10^{09}	2.54×10^{09}	2.54×10^{09}	7.05×10^{09}
$C_{(2)}+O \rightarrow CO$	TS8	9.74×10^{06}	9.74×10^{06}	9.74×10^{06}	5.39×10^{07}
$CH_3+O \rightarrow CH_3O$	TS9	1.01×10^{01}	1.01×10^{01}	1.01×10^{01}	1.00×10^{02}
$CH_2+O \rightarrow CH_2O$	TS10	1.12×10^{-01}	1.12×10^{-01}	1.12×10^{-01}	1.77×10^{00}
$CH+O \rightarrow CHO$	TS11	1.75×10^{-02}	1.75×10^{-02}	1.75×10^{-02}	7.68×10^{-01}
$O+H \rightarrow OH$	TS12	1.65×10^{07}	1.65×10^{07}	1.65×10^{07}	8.68×10^{07}
$H_2O \rightarrow OH+H$	TS13	1.55×10^{03}	1.93×10^{04}	6.34×10^{04}	2.68×10^{04}
$OH \rightarrow O+H$	TS14	5.73×10^{06}	5.73×10^{06}	5.73×10^{06}	1.64×10^{07}
$H+H \rightarrow H_2$	TS15	1.54×10^{11}	1.54×10^{11}	1.54×10^{11}	2.81×10^{11}
$CH_4+O \rightarrow CH_3+OH$	TS16	1.63×10^{02}	1.77×10^{03}	5.12×10^{03}	1.04×10^{04}
$CH_4+O \rightarrow CH_3O+H$	TS17	1.93×10^{04}	2.09×10^{05}	6.03×10^{05}	5.23×10^{05}

Micro-kinetics

Example: The rate equation of dry reforming of CH_4

Such as shown in Figure S2 and Figure S4, the highest points in energy profile of reforming of CH_4 with CO_2 and H_2O at 873K are the transition state of CO_2 and CH_4 dissociation, respectively. For example: the micro-kinetic model of dry reforming of CH_4 with Gibbs free energy is listed as follows: firstly, CO_2 molecule adsorbs on the surface (Eq. 1); and then dissociation on site (Eq. 2);

$CO_2 + * \rightarrow CO_2*$ Eq. 1

$CO_2* + * \rightarrow CO* + O_{(1)}$ Eq. 2

The rate equation of Eq.2 can be expressed as equation (1):

$$r = r_2 = k_2\left[CO_2{}^*\right][\,*\,] \quad (1)$$

Where k_2 is the rate constant of CO_2 dissociation. Since all the other steps are assumed to be in quasi-equilibrium, so [$CO_2{}^*$] can be expressed as equations (3):

$$k_+\left[CO_2\right][\,*\,] = k_-\left[CO_2{}^*\right] \quad (2)$$

$$\left[CO_2{}^*\right] = \frac{k_+[CO_2][\,*\,]}{k_-} = K_1[CO_2][\,*\,] \quad (3)$$

Where K1 is the equilibrium constant of CO_2 adsorption and desorption. So Substitute the equations (3) to (1), we can get the rate equation dry reforming of CH_4, which the result is consistent with our thermodynamics.

$$r = k_2K_1[CO_2][\,*\,] \quad (4)$$

Table S2. Computed activation energy (E_a, eV) and reaction energy (ΔH, eV) of individual elementary reactions on the Ni(111) surface reported in literature along with the computational methods

Reactions	E_a	ΔH	Methods
$CO_2 \rightarrow CO+O$	0.48	–0.82	GGA-BEEF-vdw[1]
	0.61	–1.04	GGA-PW91[2]
	0.55	–0.36	GGA-PBE[3]
	0.78	–1.02	GGA-PBE[4]
	0.45	–1.02	GGA-PBE[5]
	0.47	–1.08	GGA-PBE-D3[6]
$CH_4 \rightarrow CH_3+H$	1.21	0.55	GGA- BEEF-vdw[1]
	1.14	0.49	GGA-RPBE[7]
	1.17	0.36	GGA-PBE[3]
$CH_3 \rightarrow CH_2+H$	0.87	0.33	GGA- BEEF-vdw[1]
	0.73	–0.22	GGA-RPBE[7]
	0.82	0.29	GGA-PBE[3]
$CH_2 \rightarrow CH+H$	0.43	–0.16	GGA- BEEF-vdw[1]
	0.25	–0.55	GGA-RPBE[7]
	0.37	0.29	GGA-PBE[3]
$CH \rightarrow C+H$	1.45	0.64	GGA- BEEF-vdw[1]
	1.17	0.30	GGA-RPBE[7]
	1.37	1.21	GGA-PBE[3]
$H_{2(g)} \rightarrow 2H$	0.25	–0.88	GGA-RPBE[7]
$H_2O \rightarrow OH+H$	1.00	–0.19	GGA- BEEF-vdw[8]
	0.97	–0.22	GGA-PBE[9]
$OH \rightarrow O+H$	1.31	0.09	GGA- BEEF-vdw[8]
	1.19	–0.17	GGA-PBE[9]
$CH_4+O \rightarrow CH_3+OH$	1.66	0.54	GGA- BEEF-vdw[1]
$CH_3+O \rightarrow CH_3O$	0.94	–0.53	GGA-PBE[3]
$CH_2+O \rightarrow CH_2O$	0.78	–0.25	GGA-PBE[3]
$CH+O \rightarrow CHO$	1.13	0.41	GGA- BEEF-vdw[1]
	0.80	–0.51	GGA-PBE[3]
$C+O \rightarrow CO$	1.30	–1.72	GGA- BEEF-vdw[1]
	0.64	–2.51	GGA-PBE[3]

References

1 J. Niu, J. Ran and D. Chen, *Appl. Surf. Sci.*, 2020, **513**, 145840-145850.
2 M.-C. Silaghi, A. Comas-Vives and C. Copéret, *ACS Catal.*, 2016, **6**, 4501-4505.
3 S.-G. Wang, X.-Y. Liao, J. Hu, D.-B. Cao, Y.-W. Li, J. Wang and H. Jiao, *Surf. Sci.*, 2007, **601**, 1271-1284.
4 S.-G. Wang, D.-B. Cao, Y.-W. Li, J. Wang and H. Jiao, *J. Phys. Chem. B*, 2006, **110**, 9976-9983.
5 J. Huang, X. Li, X. Wang, X. Fang, H. Wang and X. Xu, *J. CO_2 Util.*, 2019, **33**, 55-63.
6 P. Wu, Y. Tao, H. Ling, Z. Chen, J. Ding, X. Zeng, X. Liao, C. Stampfl and J. Huang, *ACS Catal.*, 2019, **9**, 10060-10069.
7 J. Li, E. Croiset and L. Ricardez-Sandoval, *Chem. Phys. Lett.*, 2015, **639**, 205-210.
8 J. Niu, Y. Wang, Y. Qi, A. H. Dam and D. Chen, *Fuel*, 2020, **266**, 117143-117154.
9 L. Zhu, C. Liu, X. Wen, Y.-W. Li and H. Jiao, *Catal. Sci. Technol.*, 2019, **9**, 199-212.